NF B-sensitive Orai1 expression in the regulation of FGF23 release

Zhang, Bingbing ; Yan, Jing ; Umbach, Anja T ; Fakhri, Hajar ; Fajol, Abul ; Schmidt, Sebastian ; Salker, Madhuri S ; Chen, Hong ; Alexander, Dorothea ; Spichtig, Daniela ; Daryadel, Arezoo ; Wagner, Carsten A ; Föller, Michael ; Lang, Florian

Abstract: Fibroblast growth factor (FGF23) plasma levels are elevated in cardiac and renal failure and correlate with poor clinical prognosis of those disorders. Both disorders are associated with inflammation and activation of the inflammatory transcription factor NF B. An excessive FGF23 level is further observed in Klotho-deficient mice. The present study explored a putative sensitivity of FGF23 expression to transcription factor NF B, which is known to upregulate Orai1, the Ca(2+) channel accomplishing store-operated Ca(2+) entry (SOCE). In osteoblastic cells (UMR106) and immortalized primary periosteal (IPO) cells, protein abundance was determined by Western blotting, and in UMR106 cells, transcript levels were quantified by RT-PCR, cytosolic Ca(2+) activity utilizing Fura-2-fluorescence, and SOCE from Ca(2+) entry following store depletion by thapsigargin. As a result, UMR106 and IPO cells expressed Ca(2+) channel Orai1. SOCE was lowered by NF B inhibitor wogonin as well as by Orai1 inhibitors 2-APB and YM58483. UMR106 cell Fgf23 transcripts were increased by stimulation of SOCE and Ca(2+) ionophore ionomycin and decreased by Orai inhibitors 2-APB, YM58483 and SKF96365, by Orai1 silencing, as well as by NF B inhibitors wogonin, withaferin A, and CAS 545380-34-5. In conclusion, Fgf23 expression is upregulated by stimulation of NF B-sensitive, store-operated Ca(2+) entry. KEY MESSAGES Osteoblast UMR106 and IPO cells express Ca(2+) channel Orai1. Osteoblast store-operated Ca(2+) entry is accomplished by NF B-sensitive Orai1. Osteoblast Fgf23 transcription is upregulated by increase in the cytosolic Ca(2+) activity. Fgf23 transcription is decreased by Orai inhibitors and Orai1 silencing. Fgf23 transcription is lowered by NF B inhibitors.

DOI: https://doi.org/10.1007/s00109-015-1370-3

Aldosterone-sensitive NFκB-dependent Orai1 expression in the regulation of FGF23 release

Bingbing Zhang[1] PhD stud., Jing Yan[1] PhD stud., Anja T. Umbach[1] MD student, Hajar Fakhri[1] MD student, Abul Fajol[1] PhD stud., Sebastian Schmidt[1] MD, Madhuri S Salker[1] MD, Hong Chen[1] PhD stud., Dorothea Alexander[2] PhD, Daniela Spichtig[3] PhD stud., Arezoo Daryadel[3] PhD, Carsten A Wagner[3] MD, Michael Föller[4] MD, PhD, Florian Lang[1] MD

[1]Departments of Physiology, University of Tübingen, Gmelinstr. 5, 72076 Tübingen, Germany
[2]Department of Oral and Maxillofacial Surgery, University Hospital of Tübingen, Osianderstr. 2-8, 72076 Tuebingen, Germany
[3]Institute of Physiology, University of Zürich, Winterthurerstr. 190, CH-8057 Zürich, Switzerland and NCCR Kidney, CH, Switzerland
[4]Institute of Agricultural and Nutritional Sciences, Martin Luther University Halle-Wittenberg, Von-Danckelmann-Platz 2, 06120 Halle (Saale), Germany

Correspondence to:
Prof. Dr. Florian Lang
Physiologisches Institut der Universität Tübingen, Gmelinstr. 5, D-72076 TÜBINGEN
Tel: +49 7071 29 72194, Fax: +49 7071 29 5618, e-mail: florian.lang@uni-tuebingen.de

short title: Orai1-dependent regulation of FGF23

Abstract

Fibroblast growth factor (FGF23) plasma levels are elevated in cardiac and renal failure, and correlate with poor clinical prognosis of those disorders. Both disorders are associated with hyperaldosteronism. An excessive FGF23 level and hyperaldosteronism are further observed in Klotho-deficient mice. The present study explored a putative aldosterone sensitivity of FGF23 transcription and secretion and the putative involvement of transcription factor NFκB, which is known to upregulate Orai1, the Ca^{2+} channel accomplishing store operated Ca^{2+} entry (SOCE). Serum FGF23 levels were determined by ELISA in mice with or without deoxycorticosterone acetate (DOCA) treatment or salt depletion. In osteoblastic cells (UMR106) and immortalized primary periosteal (IPO) cells protein abundance was determined by Western blotting, and in UMR106 cells transcript levels were quantified by RT-PCR, cytosolic Ca^{2+}-activity utilizing Fura-2-fluorescence, and SOCE from Ca^{2+} entry following store depletion by thapsigargin. As a result, DOCA treatment and salt depletion of mice elevated the serum C-terminal FGF23 concentration. In UMR106 cells aldosterone increased Fgf23 transcript levels, an effect reversed by mineralocorticoid receptor blockers spironolactone and eplerenone, NFκB-inhibitor withaferin A, and Ca^{2+}-channel blocker YM58483. Aldosterone enahnced and spironolactone decreased Ca^{2+} entry in UMR106 cells. UMR106 and IPO cells expressed Ca^{2+}-channel Orai1. SOCE was lowered by NFκB inhibitor wogonin and blunted by Orai1 inhibitors 2-APB and YM58483. UMR106 cell Fgf23 transcripts were increased by stimulation of SOCE and Ca^{2+} ionophore ionomycin and decreased by Orai inhibitors, by Orai1 silencing, as well as NFκB inhibitors wogonin and withaferin A. In conclusion, Fgf23 expression is up-regulated by aldosterone and stimulation of NFκB-sensitive, store-operated Ca^{2+} entry.

Key words:
$1,25(OH)_2D_3$; SOCE, calcium, Orai1, NFκB

Introduction

FGF23 (fibroblast growth factor 23), a hormone released mainly from bone, is a powerful regulator of calcium phosphate metabolism [1]. FGF23 down-regulates renal 1α hydroxylase (Cyp27b1) and up-regulates 25-hydroxyvitamin D 24-hydroxylase (Cyp24a1) thus reducing the formation and enhancing the inactivation of 1,25-dihydroxyvitamin D_3 ($1,25(OH)_2D_3$) [2]. As a result, FGF23 decreases the serum level of $1,25(OH)_2$ D_3 [3, 4]. $1,25(OH)_2$ D_3 is in turn a powerful regulator of renal and intestinal phosphate and calcium transport [5, 6]. In addition to its effect on $1,25(OH)_2D_3$ formation, FGF23 directly decreases renal tubular phosphate reabsorption [3] and thus stimulates renal phosphate elimination [3]. FGF23 deficiency results in elevated serum phosphate, calcium and $1,25(OH)_2D_3$ levels with excessive vascular calcifications, rapid aging and a profound decrease of lifespan [2].

The effect of FGF23 on $1,25(OH)_2D_3$ formation requires αKlotho as a co-receptor [7, 8]. Mice lacking functional αKlotho similarly suffer from extensive vascular calcifications, early onset of multiple age-related disorders and severe shortening of life span [8]. Similar to FGF23 deficiency, αKlotho deficiency is effective mainly through excessive $1,25(OH)_2D_3$ formation, enhanced renal tubular phosphate reabsorption and increased serum phosphate levels [9]. As a matter of fact, hyperphosphatemia fosters vascular calcification [10] and is considered a predictor of mortality [11]. FGF23 plasma levels are extremely high in Klotho deficient mice, a result at least in part due to excessive $1,25(OH)_2D_3$ levels, but again paralleled by hyperaldosteronism [12, 13].

The pathophysiological role of FGF23 has, however, remained enigmatic [14, 15]. In patients with cardiac failure [16, 17], acute renal failure [18], chronic kidney disease [7, 17, 19], diabetic nephropathy [20] and hepatic failure [21], plasma FGF23 concentrations are high and associated with accelerated disease progression, morbidity and/or mortality. Mechanisms up-regulating FGF23 in those disorders are still ill-defined.

Known regulators of FGF23 release include $1,25(OH)_2D_3$ [7], αKlotho [22, 23], PHEX (phosphate-regulating gene with homology to endopeptidase), DMP-1 (dentin matrix protein or cyclin D binding myb-like protein 1), sustained phosphate load even without hyperphosphatemia, a high extracellular Ca^{2+} concentration, and PTH [7, 24]. FGF23 plasma levels are further modified by iron deficiency [25, 26], pregnancy [27] and FGF23 secreting tumors [28].

To the best of our knowledge, nothing is known about a role of the cytosolic Ca^{2+} concentration ($[Ca^{2+}]_i$) in FGF23 expression. In some cell types Ca^{2+} may enter through SOCE,

i.e. store-operated Ca^{2+} entry, which is stimulated by intracellular Ca^{2+} store depletion [29]. SOCE is accomplished by the 4-transmembrane-spanning pore forming calcium release-activated channel (CRAC) moiety Orai1 (CRACM1) [30], and its regulator stromal interaction molecule 1 (STIM1), which senses the Ca^{2+} content of the endoplasmic reticulum (ER) [31]. The expression of Orai1 has previously been shown to be regulated by nuclear transcription factor NFκB [32].

Regulators of NFκB include mineralocorticoids [33, 34]. In patients with non-ischemic cardiac disease and early chronic kidney disease high FGF23 plasma levels are associated with high plasma aldosterone concentrations [17].

The present study explored whether aldosterone modifies FGF23 release and, if so, whether the effect involves NFκB-sensitive Ca^{2+} entry.

Materials and Methods

Animal experiments

The animal experiments were conducted according to the German law for the welfare of animals and were approved by the state of Baden-Württemberg (Regierungspräsidium). To study the direct effect of mineralocorticoids on FGF23 release *in vivo*, 50 µl blood was collected from male and female C57BL/6 mice (8-20 weeks old). Then, mice were treated with a single s.c. injection of deoxycorticosterone acetate (DOCA; 100 mg/kg b.w.; Sigma, Schnelldorf, Germany) or spironolactone (75 mg/kg b.w.; Sigma) or sham-treated. Twelve hours after the injection, another 50 µl blood was collected. For the effect of the low salt diet on FGF23 release, male and female mice (2-13-month-old) were fed a control diet or a low salt diet (containing <0.2% Na^+ and Cl^-; Altromin, Lage, Germany) for a total of 7-14 days and subsequently 50 µl blood were collected. Serum C-terminal FGF23 was determined with an ELISA kit (Immutopics, San Clemente, USA). Serum aldosterone and corticosterone were quantified by means of kits from IBL (Hamburg, Germany) according to the manufacturers' protocol.

Cell culture

UMR106 rat osteosarcoma cells were cultured in DMEM high glucose medium supplemented with 10% FCS and 1% penicillin/streptomycin under standard culture conditions. Human immortalized primary periosteal cells (IPO) were cultured in DMEM F-12

(1:1 mixture of DMEM and Ham's F-12, high glucose) containing Glutamax and 10% FCS and 1% penicillin/streptomycin/1% fungizide.

Cells were pretreated with 100 nM $1,25(OH)_2D_3$ (Sigma, Schnelldorf, Germany). After 24 h cells were in addition treated with 50 µM Orai inhibitor 2-APB (TOCRIS, Bristol, UK), 100 nM Orai inhibitor YM58483 (TOCRIS), 10 µM Orai inhibitor SK&F96365 (TOCRIS), 500 nM NFκB inhibitor withaferin A (TOCRIS), or NFκB inhibitor CAS 545380-34-5 (EMD) for another 24 h or treated with vehicle only. Cells pretreated with 100 nM $1,25(OH)_2D_3$ for 46 h were incubated with or without 100 nM ionomycin (Sigma) or 500 nM thapsigargin (Sigma) for 2 h. Alternatively, cells were incubated with or without 100 µM NFκB inhibitor wogonin (Sigma). After 24 h, $1,25(OH)_2D_3$ (100 nM) was added, and cells were analyzed after another 24 h. For some experiments, cells were pretreated with 100 nM $1,25(OH)_2D_3$ for 42 h. Then, 100 nM aldosterone (Sigma) was added without or with 10 µM spironolactone, 10 µM eplerenone, 100 nM YM58483, 500 nM withaferin A, or 50 µM SGK1 inhibitor EMD638683 (Merck Darmstadt, Germany) for 6 h.

For the calcium measurements and the quantification of Orai1 transcripts, cells were treated with 100 nM aldosterone (Sigma) or 10 µM spironolactone (Sigma) for 24 h in serum-free medium. Where indicated, experiments were performed in the presence of nifedipine (100 µM) or verapamil (10 µM) (both from Sigma).

Silencing

For silencing, 1 x 10^5 cells (12-well plate) and 2 x 10^5 cells (6-well plate) were seeded 24 h before the experiment in antibiotic-free medium. Cells were transfected with 5 µl/1000 µl ON-TARGETplus RAT Orai1 siRNA (5 µM, Thermo Fisher Scientific, Waltham, MA, USA) and ON-TARGETplus Non-targeting siRNA (5 µM, Thermo Fisher Scientific) using the cationic lipid DharmaFECT 1 transfection reagent (0.5 µl/1000 µl, Thermo Fisher Scientific) according to the manufacturer's protocol. Twenty-four hours after transfection, cells were treated with $1,25(OH)_2D_3$ (100 nM) for another 24 h. Cells were then harvested and analyzed. To verify silencing efficiency, the Orai1 transcript level was quantified. As a result, the Orai1 mRNA level was 0.33 ± 0.05 a.u. (n=16) in cells transfected with a negative control siRNA and 0.13 ± 0.01 a.u. (n=16), $p<0.001$ in cells transfected with a negative control siRNA.

Quantification of mRNA expression

For the mRNA expression analysis in UMR106 cells, the final volume of the RT-PCR reaction mixture was 15 µl and contained: 1 µl cDNA, 1 µM of each primer, 7.5 µl GoTaq

Master Mix Green (Promega), and sterile water up to 15 µl. PCR conditions were 95°C for 3 min, followed by 40 cycles of 95°C for 10 s, 58°C for 30 s and 72°C for 45s. The product size was analyzed on a 2% agarose gel. Quantitative RT-PCR was performed on a BioRad iCycler iQTM Real-Time PCR Detection System (Bio-Rad Laboratories, München, Germany).

For the determination of Fgf23 transcripts in mouse bone, bone was homogenized in liquid nitrogen using mortar and pestle. Total mRNA from bone was extracted with TRIzol (Invitrogen, Switzerland) followed by purification with RNeasy Mini Kit (Qiagen, Switzerland) according to the manufacturer's protocol. DNAse digestion was performed using the RNase-free DNAase Set (Qiagen, Switzerland). Total RNA extractions were analyzed for quality, purity, and concentration using the NanoDrop ND-1000 spectrophotometer (Wilmington, Germany). RNA samples were diluted to a final concentration of 100 ng/µl and cDNA was prepared using the TaqMan Reverse Transcriptase Reagent Kit (Applied Biosystems, Roche, Foster City, CA). In brief, in a reaction volume of 40 µl, 300 ng of RNA was used as template and mixed with the following final concentrations of RT buffer (1x): $MgCl_2$ (5.5 mmol/l), random hexamers (2.5 µmol/l), dNTP mix (500 µmol/l each), RNase inhibitor (0.4 U/µl), multiscribe reverse transcriptase (1.25 U/µl), and RNAse-free water. Reverse transcription was performed with thermocycling conditions set at 25°C for 10 min, 48°C for 30 min, and 95°C for 5 min on a thermocycler (Biometra, Göttingen, Germany). Quantitative realtime PCR (RT-PCR) was performed on the ABI PRISM 7700 Sequence Detection System (Applied Biosystems). Primers were chosen to spanning intron–exon boundaries to exclude genomic DNA contamination. The specificity of all primers was tested and always resulted in a single product of the expected size (data not shown). Probes were labeled with the reporter dye FAM at the 5'-end and the quencher dye TAMRA at the 3'-end (Microsynth, Balgach, Switzerland). Real-time PCR reactions were performed using KAPA PROBE FAST qPCR Kit (KappaBiosystems, USA).

The following primers were used:

Rat Tbp (TATA box-binding protein):

forward (5'-3'): ACTCCTGCCACACCAGCC

reverse (5'-3'): GGTCAAGTTTACAGCCAAGATTCA

Rat Fgf23

forward (5'-3'): TGGCCATGTAGACGGAACAC

reverse (5'-3'): GGCCCCTATTATCACTACGGAG

Rat Orai1

forward (5'-3'): CGTCCACAACCTCAACTCC

reverse (5'-3'): AACTGTCGGTCCGTCTTAT

Rat Orai2

forward (5'-3'): GGAAGCCGTGAGCAACAT

reverse (5'-3'): CACCAGGGAGCGGTAGAA

Rat Orai3

forward (5'-3'): TTTTGGTGGGCTGGGTCA

reverse (5'-3'): TCCTGCTTGTGGCGGTCT

Rat Stim1

forward (5'-3'): CGTCCGCAACATCCACAAG

reverse (5'-3'): CCATAGGTCCTCCACGCT

Rat Stim2

forward (5'-3'): ACTTAGAAAGCCTACAAACCG

reverse (5'-3'): GCATCAGGGACAGACCAG

Rat Sgk1

forward (5'-3'): ATGTGAAGCACCCTTTCCTG

reverse (5'-3'): TAGAACAGCTCTCCGCCATT

Mouse Fgf23

forward (5'-3'): TCGAAGGTTCCTTTGTATGGAT

reverse (5'-3'): AGTGATGCTTCTGCGACAAGT

Calculated mRNA expression levels were normalized to the expression levels of Tbp (in rat derived cell lines) or HPRT/18S (in mice) of the same cDNA sample. Relative quantification of gene expression was performed using the ΔΔCt method.

Western blotting

Orai1 protein abundance was determined in UMR106 cells, IPO cells, and mouse bone (femur). The cells were washed in ice-cold PBS. For bone preparation, a mouse was sacrificed and the femur isolated. Muscles were carefully removed and the femur snap-frozen. After thawing, the epiphyses were removed and the bone marrow was flushed out with ice-cold PBS. Using a mortar and pestle, the bone was pulverized on dry ice. RIPA lysis buffer (Cell Signaling, Frankfurt, Germany) containing phosphatase and protease inhibitor cocktail tablet (Complete mini, Roche, Mannheim, Germany) was added to the washed cells or the bone powder. The samples were incubated on ice for 30 min and then centrifuged at 14,000 rpm and 4°C for 20 min. The supernatant was removed and used for Western blotting. Total protein (40-60 µg) was separated by SDS-PAGE, thereafter transferred to PVDF membranes and

blocked in 5% non-fat milk/Tris-buffered saline/Tween-20 (TBST) at room temperature for 1 hour. Membranes were probed overnight at 4ºC with polyclonal rabbit anti-Orai1 antibody (1:700 in 5% BSA in TBST; Proteintech, Manchester, UK). After incubation with horseradish peroxidase-conjugated anti-rabbit secondary antibody (Cell Signaling, Frankfurt, Germany; 1:2000) for 1 hour at room temperature, the bands were visualized with enhanced chemiluminescence reagents (Amersham, Freiburg, Germany). Membranes were also probed with GAPDH antibody (Cell signaling, 1:2000) as loading control. Densitometric analysis was performed using quantity One software (Bio-Rad, München, Germany).

Measurement of intracellular Ca^{2+}

To determine the cytosolic Ca^{2+} concentration ($[Ca^{2+}]_i$), UMR106 cells were loaded with Fura-2/AM (2 µM, Molecular Probes, Göttingen, Germany) for 15 min at 37°C. Fluorescence measurements were carried out with an inverted phase-contrast microscope (Axiovert 100, Zeiss, Oberkochen, Germany). Cells were excited alternatively at 340 or 380 nm and the light was deflected by a dichroic mirror into either the objective (Fluar 40×/1.30 oil, Zeiss, Oberkochen, Germany) or a camera (Proxitronic, Bensheim, Germany). Emitted fluorescence intensity was recorded at 505 nm. Data acquisition was accomplished by using specialized computer software (Metafluor, Universal Imaging Downingtown, USA). As a measure for the increase in the cytosolic Ca^{2+} concentration, the slope and peak of the changes in the 340/380 nm ratio were determined in each experiment.

To determine SOCE, intracellular Ca^{2+} was measured before and after removal of extracellular Ca^{2+} (and addition of 0.5 mM EDTA), followed by addition of thapsigargin (1 µM) and subsequent readdition of extracellular Ca^{2+} to Ringer solution, composed of (in mM): 125 NaCl, 5 KCl, 1.2 $MgSO_4$, 32.2 HEPES, 2 Na_2HPO_4, 0 or 2 $CaCl_2$ and 0.5 or 0 EGTA, respectively, and 5 glucose, pH 7.4 (NaOH).

Immunofluorescence

UMR106 cells treated with 100 nM aldosterone were cultured on 4-well chamber slides (Thermo scientific), washed, and fixed with 4% paraformaldehyde for 30 min at room temperature. For blocking unspecific bindings, UMR106 cells were incubated with 3% Albumin Fraction V (Carl Roth, Karlsruhe, Germany), 5% normal goat serum (Sigma, Schnelldorf, Germany), and 0.5% Triton in PBS (PAA, Cölbe, Germany) for 30 min at room temperature. Then, the cells were exposed to rabbit anti-p65 (1:1000, Genetex, Irvine, USA) at 4°C in a humidified chamber overnight. The cells were rinsed four times with PBS and

incubated with DyLight® 488-conjugated goat anti-rabbit antibody (1:3000, BIOZOL, Eching, Germany) for 1 h at room temperature. After four washing steps the nuclei were stained with DRAQ-5 dye (1:400; BIOZOL) for 30 min at room temperature. The slides and coverslips were mounted with FluorSave™ Reagent (Calbiochem, Darmstadt, Germany). Images were taken on a LSM 5 EXCITER confocal laser scanning microscope (Zeiss, Germany) with a water-immersion Plan-Neofluar 40×/1.3 NA differential interference contrast and analyzed with the instrument's software.

Statistics

Data are provided as means ± SEM, *n* represents the number of independent experiments. All data were tested for significance using unpaired Student *t*-test or ANOVA. Only results with $p < 0.05$ were considered statistically significant.

Results

The present study explored whether FGF23 release is triggered by mineralocorticoids, and, if so, whether the effect involves NFκB-sensitive Ca^{2+} signaling.

In order to test for an effect of mineralocorticoids on FGF23 release, a single dose of DOCA (100 mg/kg b.w. s.c.) or vehicle was injected into wild type mice and 12 hours later the serum C-terminal FGF23 (cFGF23) levels determined. As illustrated in Fig. 1A, the injection of DOCA was followed by a marked and significant increase in the serum cFGF23 concentration. In a second series of experiments, mice were fed a low salt diet. As expected, this diet induced an elevation of the serum aldosterone level (889 ± 217 pg/ml; n=5) compared to standard chow-fed mice (268 ± 27 pg/ml; n=5; p<0.01). The diet did not significantly affect the serum corticosterone level (low salt diet: 162 ± 32 ng/ml; n=5; standard chow: 120 ± 31 ng/ml; n=5). As illustrated in Fig 1B, the low salt diet elevated the serum concentration of C-terminal FGF23. The main site of FGF23 formation is the bone. Accordingly, we found a higher level of Fgf23 transcripts in bone from DOCA-treated mice compared to untreated mice (Fig. 1C). Treatment with spironolactone (12 h, 75 mg/kg b.w.) did, however, not significantly influence the serum FGF23 concentration (control: 201 ± 6 pg/ml, n=5; spironolactone: 332 ± 65 pg/ml, n=5). Similarly, spironolactone treatment did not block the increase in serum FGF23 induced by low-salt diet (serum FGF23 before low-salt diet: 134 ± 15 pg/ml; serum FGF23 after two weeks of low-salt diet: 194 ± 13 pg/ml; n=8; p<0.01).

The next series of experiments explored whether Ca^{2+} release-activated Ca^{2+}-channel (CRAC) moiety Orai1 and its regulator STIM1 are expressed in osteoblastic cells and therefore participate in the signaling regulating FGF23 formation in those cells. Experiments were thus performed in UMR106 osteoblast-like cells and in immortalized primary periosteal cells (IPO). As illustrated in Fig.2A, Orai1 was expressed in UMR106 and IPO cells as well as in bone. Moreover, Orai3 and STIM2 transcripts could be readily detected in UMR106 cells whereas the abundance of Orai2 and Stim1 was low (Fig. 2B). Orai1 transcript levels were reduced following inhibition of NFκB by wogonin in UMR106 cells (Fig. 2C).

Fluorescence optics was employed to explore whether Orai1 and/or NFκB impact on intracellular Ca^{2+} concentration ($[Ca^{2+}]_i$). Store-operated Ca^{2+} entry (SOCE) requires depletion of intracellular Ca^{2+} stores which was accomplished by inhibition of the sarcoendoplasmic Ca^{2+} ATPase (SERCA) with thapsigargin (1 μM) in the absence of extracellular Ca^{2+}. SOCE was estimated from the increase in $[Ca^{2+}]_i$ following re-addition of extracellular Ca^{2+}. As illustrated in Fig. 3A,D,G,J, thapsigargin (10 μM) treatment in the absence of extracellular Ca^{2+} was followed by a transient elevation of $[Ca^{2+}]_i$ reflecting depletion of intracellular stores. The subsequent addition of extracellular Ca^{2+} was followed by a rapid increase in $[Ca^{2+}]_i$ reflecting store-operated Ca^{2+} entry (SOCE). Addition of Orai1 inhibitors 2-APB (Fig. 3A-C) or YM58483 (Fig. 3D-F) did not significantly modify the thapsigargin-induced increase in $[Ca^{2+}]_i$ but virtually abrogated the increase in $[Ca^{2+}]_i$ following re-addition of extracellular Ca^{2+}. Similarly, Orai1 silencing did not significantly modify the thapsigargin-induced increase in $[Ca^{2+}]_i$ but significantly blunted the increase in $[Ca^{2+}]_i$ following re-addition of extracellular Ca^{2+} (Fig. 3G-I). Exposure of UMR106 cells to wogonin significantly blunted the thapsigargin-induced increase in $[Ca^{2+}]_i$ and the increase in $[Ca^{2+}]_i$ following re-addition of extracellular Ca^{2+} (Fig. 3J-L). Similarly, the NFκB inhibitor CAS 545380-34-5 decreased Orai1 transcript levels, the thapsigargin-induced increase in $[Ca^{2+}]_i$ and SOCE in UMR106 cells (suppl. Fig. 1A and C).

Next, RT-PCR was employed to determine whether Ca^{2+} entry and/or NFκB influences the formation of FGF23. As illustrated in Fig, 4, Fgf23 transcript levels were significantly increased by the Ca^{2+} ionophore ionomycin (Fig. 4A) and by thapsigargin (Fig. 4B). Conversely, blocking Ca^{2+} entry by the Orai blockers 2-ABP (Fig. 4C), YM58483 (Fig. 4D), or SK&F96365 (Fig. 4E) decreased the abundance of Fgf23 transcripts. In view of the limited specificity of the Orai1 blockers, additional experiments were performed with silencing of Orai1. As illustrated in Fig. 4F, silencing of Orai1 also lowered FGF23 transcript levels in UMR106 cells. We could, however, not confirm a significant decrease of Orai1 protein abundance following Orai1 silencing (data not shown). Nevertheless, steady-state FGF23

production in UMR106 cells was dependent on $[Ca^{2+}]_i$ which was modified by Ca^{2+} entry. In contrast, L-type calcium channel inhibitors did not appreciably influence FGF23 transcript levels. The Fgf23 transcript level was 0.019 ± 0.004 a.u. in control cells (n=9) and 0.018 ± 0.003 a.u. (n=9) in cells treated with L-type channel inhibitor nifedipine (100 µM, 24 h). In another series, the Fgf23 transcript level was 0.011 ± 0.001 a.u. (n=9) in control cells and 0.011 ± 0.001 a.u. (n=9) in cells treated with L-type channel inhibitor verapamil (10 µM, 24 h).

Since Ca^{2+} entry into UMR106 cells could be attenuated by the NFκB inhibitor wogonin (Fig. 3J-L), we tested whether FGF23 formation is also NFκB-sensitive. Indeed, Fgf23 transcript levels were reduced by the NFκB inhibitors wogonin (Fig. 5A) and withaferin A (Fig. 5B). The NFκB inhibitor CAS 545380-34-5 also decreased FGF23 transcript levels (suppl. Fig 1B*)*.

Since the level of confluence has been shown to affect FGF23 production in primary osteoblasts [35], we preformed experiments at different stages of confluency. In a culture of 300,000 UMR106 cells, the FGF23 transcript levels were significantly ($p<0.01$) higher in control cells (0.029 ± 0.005 a.u., n=12) than in cells exposed 24 hours to 100 µM wogonin (0.009 ± 0.001 a.u., n=12). In a culture of 200,000 UMR106 cells, the FGF23 transcript level were again significantly ($p<0.001$) higher in control cells (0.012 ± 0.001 a.u., n=12) than in cells exposed for 24 hours to 100 µM wogonin (0.004 ± 0.000 a.u., n=12). Finally, in a culture of 100,000 UMR106 cells, the FGF23 transcript level was again significantly ($p<0.01$) higher in control cells (0.006 ± 0.001 a.u., n=12) than in cells exposed 24 hours to 100 µM wogonin (0.002 ± 0.000 a.u., n=12). Thus, the level of confluence influenced the basal FGF23 transcript level but did not affect the inhibitory effect of wogonin on FGF23 formation.

To test whether aldosterone influences Ca^{2+} signaling, UMR106 cells were treated with aldosterone or the mineralocorticoid receptor antagonist spironolactone and intracellular Ca^{2+} concentrations ($[Ca^{2+}]_i$) were determined prior to and following removal of extracellular Ca^{2+}, addition of thapsigargin, and re-addition of extracellular Ca^{2+}. As illustrated in Fig. 6A-C, aldosterone did not significantly modify the thapsigargin-induced increase in $[Ca^{2+}]_i$ but significantly enhanced the elevation of $[Ca^{2+}]_i$ following re-addition of extracellular Ca^{2+}. Conversely, spironolactone did not significantly modify the thapsigargin-induced increase in $[Ca^{2+}]_i$ either, but significantly blunted the increase in $[Ca^{2+}]_i$ following re-addition of extracellular Ca^{2+} (Fig. 6D-F).

A final series of experiments explored whether the influence of aldosterone and spironolactone on Ca^{2+} signaling in UMR106 cells was involved in the transcriptional regulation of Fgf23. Aldosterone (Fig. 7A) significantly elevated the Orai1 transcript level in

UMR106 cells. Moreover, aldosterone up-regulated the transcription of Fgf23, an effect virtually abrogated by spironolactone, the Orai inhibitor YM58483, or the NFκB inhibitor withaferin A (Fig. 7B). The dose-response curve of the aldosterone effect on FGF23 is shown in Fig 7C. The aldosterone antagonist eplerenone similarly reversed the aldosterone effect on Fgf23 (Fig. 7D). Immunofluorescence confirmed activation of NFκB by aldosterone in UMR106 cells (Fig. 7E).

A possible mediator of the aldosterone effect on Orai1 is SGK1 which has been shown to up-regulate this channel. Employing qRT-PCR we indeed found a positive effect of aldosterone on the Sgk1 transcript level in UMR106 cells (control: 0.73 ± 0.04 a.u., n=12; 100 nM aldosterone: 1.02 ± 0.05 a.u.,n=12; $p<0.001$). Moreover, aldosterone failed to stimulate FGF23 expression in the presence of a SGK1 inhibitor (Fig. 7F).

The dose effects of mineralocorticoid antagonism with spironolactone or eplerenone are displayed in Fig. 8A and 8B, respectively. Notably, the effect of higher aldosterone concentrations on FGF23 transcription were also blocked by the glucocorticoid antagonist mifepristone (Fig. 8C).

Discussion

The present observations reveal that mineralocorticoids may contribute to the regulation of FGF23 transcription and release. Furthermore, they disclose a decisive role of the cytosolic Ca^{2+} concentration ($[Ca^{2+}]_i$) for the regulation of FGF23 release. Store operated Ca^{2+} entry (SOCE) apparently stimulated the transcription of Fgf23. SOCE is accomplished by the pore-forming Orai (CRAC) isoforms [30] and their regulators STIM1 and STIM2 [31]. According to the present observations, Orai1 and STIM2 are both highly expressed in osteoblastic UMR106 cells. Orai1 expression has been shown to be up-regulated by the transcription factor NFκB [32]. Our study demonstrates that in UMR106 cells inhibition of NFκB reduced Orai1 transcript levels. Moreover, Fgf23 expression was also down-regulated by NFκB inhibitors. Aldosterone has previously been shown to up-regulate NFκB [33, 36]. The present study reveals that the effect of aldosterone is abrogated by NFκB inhibitors. The present observations do, however, not rule out that NFκB plays a permissive role in the regulation of FGF23 expression and release. Moreover, we cannot rule out that Ca^{2+} entry mechanisms other than Orai1 are involved in the stimulation of FGF23 transcription.

As aldosterone is effective at concentrations as low as 1 nM, the effect of aldosterone is most likely in part due to stimulation of mineralocorticoid receptors. The effect of higher

aldosterone concentrations is, however, blunted by the glucocorticoid antagonist mifepristone, an observation pointing to effects of glucocorticoid receptors. Noteworthy, both, mineralocorticoid and glucocorticoid receptors upregulate the serum & glucocorticoid inducible kinase (SGK1) which has been shown to upregulate Orai1 dependent Ca^{2+} entry by activating NFκB [37]. Along those lines, pharmacological SGK1 inhibition reversed the effect of aldosterone on FGF23 expression. Spironolactone treatment, however, did not reverse the increase in serum FGF23 induced by low-salt diet. Thus, the possibility must be kept in mind that mechanisms other than mineralocorticoid receptor activation contribute to the up-regulation of FGF23 release during dehydration. Along those lines, renal klotho expression is not only down-regulated by mineralocorticoids but as well by ADH [38].

Chronic kidney disease [39-41], heart failure [42-44], diabetic nephropathy [45] and hepatic failure [44] are all characterized by hyperaldosteronism. According to the present observations, the high FGF23 plasma concentration in heart failure [16, 17], acute renal failure [18], chronic kidney disease [7, 17, 19], diabetic nephropathy [20] and hepatic failure [21] could at least in part be secondary to the hyperaldosteronism associated with those diseases. Orai1 is up-regulated by the SGK1 [32], which is in turn markedly up-regulated by aldosterone and during diabetes [46].

FGF23 is further high in polycystic kidney disease [14]. It is therefore tempting to speculate that the excessive FGF23 plasma level in polycystic kidney disease results from NFκB-dependent up-regulation of Orai1. FGF23 levels are also high in gene targeted mice expressing WNK-resistant SPAK [47] or OSR1 [48] an effect possibly also due to renal sodium wasting and thus increased release of aldosterone.

The FGF23 and aldosterone serum level is further elevated in Klotho-deficient mice [12, 13]. According to the present observations, the hyperaldosteronism of those mice could contribute to excessive FGF23 formation. It should be pointed out, however, that the FGF23 level is most likely in large part due to stimulation of FGF23 formation by high $1,25(OH)_2D_3$.

The regulation of FGF23 formation by NFκB and Ca^{2+} entry is expected to influence mineral metabolism. FGF23 down-regulates renal 1α hydroxylase expression and thus the formation of $1,25(OH)_2D_3$ [49, 50] as it requires αKlotho as a co-receptor for its effect on $1,25(OH)_2D_3$ formation [8]. $1,25(OH)_2\ D_3$ is known to stimulate both, renal and intestinal phosphate transport [5]. Moreover, FGF23 reduces renal tubular phosphate reabsorption more directly by inhibiting proximal tubular Na^+-coupled phosphate transport [50]. FGF23 thus fosters phosphaturia and hypophosphatemia. In chronic kidney disease hyperphosphatemia results in vascular calcifications [51] and both, Klotho and FGF23 counteract those

calcifications [39]. As a high serum phosphate concentration triggers vascular calcifications and is associated with accelerated aging and a decreased life span [52], high FGF23 plasma levels protect against vascular calcifications, aging and early death. Along those lines, αKlotho [53] and FGF23 [54] counteract aging and lack of either, αKlotho [53] or FGF23 [50] fosters early appearance of multiple age-related disorders leading to early death. $1,25(OH)_2D_3$ stimulates the release of FGF23 [24] and thus triggers a negative feedback loop limiting $1,25(OH)_2D_3$ formation.

The pathophysiological impact of elevated FGF23 plasma levels is still ill-defined. While a high FGF23 plasma level is associated with high morbidity and mortality in heart and kidney failure [16-18], FGF23 neutralization increases the mortality of rats with chronic kidney disease-mineral and bone disorder [55]. In view of the present observations it is tempting to speculate that the association between the FGF23 plasma level and morbidity and mortality reflects the stimulating effect of aldosterone and/or NFκB on inflammation on the one side and FGF23 formation on the other, thus affecting both, FGF23 plasma level and disease progression.

In conclusion, the present observations disclose a novel mechanism regulating FGF23 release. FGF23 formation in UMR106 cells is stimulated by an increased cytosolic Ca^{2+} concentration, which is regulated by store operated Ca^{2+} entry (SOCE). SOCE and FGF23 formation are up-regulated by the transcription factor NFκB. Aldosterone up-regulates FGF23 by NFκB and SOCE sensitive cellular mechanisms.

Acknowledgements

The authors acknowledge the technical assistance of E. Faber.

The study was supported by the Deutsche Forschungsgemeinschaft (La 315/15-1, Fo 695/1-1 and Fo 695/1-2) and the National Center for Competence in Research NCCR Kidney.CH financed by the Swiss National Science Foundation.

All authors disclose that they have no potential conflict of interest (e.g., consultancies, stock ownership, equity interests, patent-licensing arrangements, lack of access to data, or lack of control of the decision to publish).

References

1. Hori M, Shimizu Y, Fukumoto S (2011) Minireview: fibroblast growth factor 23 in phosphate homeostasis and bone metabolism. Endocrinology 152: 4-10
2. Shimada T, Kakitani M, Yamazaki Y, Hasegawa H, Takeuchi Y, Fujita T, Fukumoto S, Tomizuka K, Yamashita T (2004) Targeted ablation of Fgf23 demonstrates an essential physiological role of FGF23 in phosphate and vitamin D metabolism. J Clin Invest 113: 561-568
3. Bai X, Miao D, Li J, Goltzman D, Karaplis AC (2004) Transgenic mice overexpressing human fibroblast growth factor 23 (R176Q) delineate a putative role for parathyroid hormone in renal phosphate wasting disorders. Endocrinology 145: 5269-5279
4. Saito H, Kusano K, Kinosaki M, Ito H, Hirata M, Segawa H, Miyamoto K, Fukushima N (2003) Human fibroblast growth factor-23 mutants suppress Na+-dependent phosphate co-transport activity and 1alpha,25-dihydroxyvitamin D3 production. J Biol Chem 278: 2206-2211
5. Brown AJ, Finch J, Slatopolsky E (2002) Differential effects of 19-nor-1,25-dihydroxyvitamin D(2) and 1,25-dihydroxyvitamin D(3) on intestinal calcium and phosphate transport. J Lab Clin Med 139: 279-284
6. Murer H, Hernando N, Forster I, Biber J (2000) Proximal tubular phosphate reabsorption: molecular mechanisms. Physiol Rev 80: 1373-1409
7. Hu MC, Shiizaki K, Kuro-o M, Moe OW (2013) Fibroblast growth factor 23 and Klotho: physiology and pathophysiology of an endocrine network of mineral metabolism. Annu Rev Physiol 75: 503-533
8. Kuro-o M (2010) Overview of the FGF23-Klotho axis. Pediatr Nephrol 25: 583-590
9. Hu MC, Shi M, Zhang J, Pastor J, Nakatani T, Lanske B, Razzaque MS, Rosenblatt KP, Baum MG, M K-o, et al. (2010) Klotho: a novel phosphaturic substance acting as an autocrine enzyme in the renal proximal tubule. FASEB J 24: 3438-3450
10. Giachelli CM (2003) Vascular calcification: in vitro evidence for the role of inorganic phosphate. J Am Soc Nephrol 14: S300-S304
11. Tonelli M, Sacks F, Pfeffer M, Gao Z, Curhan G (2005) Relation between serum phosphate level and cardiovascular event rate in people with coronary disease. Circulation 112: 2627-2633
12. Fischer SS, Kempe DS, Leibrock CB, Rexhepaj R, Siraskar B, Boini KM, Ackermann TF, Foller M, Hocher B, Rosenblatt KP, et al. (2010) Hyperaldosteronism in Klotho-deficient mice. Am J Physiol Renal Physiol 299: F1171-1177
13. Voelkl J, Alesutan I, Leibrock CB, Quintanilla-Martinez L, Kuhn V, Feger M, Mia S, Ahmed MS, Rosenblatt KP, Kuro OM, et al. (2013) Spironolactone ameliorates PIT1-dependent vascular osteoinduction in klotho-hypomorphic mice. J Clin Invest 123: 812-822
14. Lang F, Föller M (2014) Enigmatic Cassandra: renal FGF23 formation in polycystic kidney disease. Kidney Int 85: 1260-1262
15. Moe OW (2012) Fibroblast growth factor 23: friend or foe in uremia? J Clin Invest 122: 2354-2356
16. Faul C, Amaral AP, Oskouei B, Hu MC, Sloan A, Isakova T, Gutierrez OM, Aguillon-Prada R, Lincoln J, Hare JM, et al. (2011) FGF23 induces left ventricular hypertrophy. J Clin Invest 121: 4393-4408

17. Imazu M, Takahama H, Asanuma H, Funada A, Sugano Y, Ohara T, Hasegawa T, Asakura M, Kanzaki H, Anzai T, et al. (2014) Pathophysiological Impact of Serum Fibroblast Growth Factor 23 in Patients with Non-ischemic Cardiac Disease and Early Chronic Kidney Disease. Am J Physiol Heart Circ Physiol 10.1152/ajpheart.00331.2014: ajpheart 00331 02014
18. Christov M (2014) Fibroblast growth factor 23 in acute kidney injury. Curr Opin Nephrol Hypertens 23: 340-345
19. Evenepoel P, Meijers B, Viaene L, Bammens B, Claes K, Kuypers D, Vanderschueren D, Vanrenterghem Y (2010) Fibroblast growth factor-23 in early chronic kidney disease: additional support in favor of a phosphate-centric paradigm for the pathogenesis of secondary hyperparathyroidism. Clin J Am Soc Nephrol 5: 1268-1276
20. Zanchi C, Locatelli M, Benigni A, Corna D, Tomasoni S, Rottoli D, Gaspari F, Remuzzi G, Zoja C (2013) Renal expression of FGF23 in progressive renal disease of diabetes and the effect of ace inhibitor. PLoS One 8: e70775
21. Prie D, Forand A, Francoz C, Elie C, Cohen I, Courbebaisse M, Eladari D, Lebrec D, Durand F, Friedlander G (2013) Plasma fibroblast growth factor 23 concentration is increased and predicts mortality in patients on the liver-transplant waiting list. PLoS One 8: e66182
22. Juppner H, Wolf M (2012) alphaKlotho: FGF23 coreceptor and FGF23-regulating hormone. J Clin Invest 122: 4336-4339
23. Smith RC, O'Bryan LM, Farrow EG, Summers LJ, Clinkenbeard EL, Roberts JL, Cass TA, Saha J, Broderick C, Ma YL, et al. (2012) Circulating alphaKlotho influences phosphate handling by controlling FGF23 production. J Clin Invest 122: 4710-4715
24. Masuyama R, Stockmans I, Torrekens S, Van Looveren R, Maes C, Carmeliet P, Bouillon R, Carmeliet G (2006) Vitamin D receptor in chondrocytes promotes osteoclastogenesis and regulates FGF23 production in osteoblasts. J Clin Invest 116: 3150-3159
25. Clinkenbeard EL, Farrow EG, Summers LJ, Cass TA, Roberts JL, Bayt CA, Lahm T, Albrecht M, Allen MR, Peacock M, et al. (2014) Neonatal iron deficiency causes abnormal phosphate metabolism by elevating FGF23 in normal and ADHR mice. J Bone Miner Res 29: 361-369
26. Wolf M, Koch TA, Bregman DB (2013) Effects of iron deficiency anemia and its treatment on fibroblast growth factor 23 and phosphate homeostasis in women. J Bone Miner Res 28: 1793-1803
27. Kirby BJ, Ma Y, Martin HM, Buckle Favaro KL, Karaplis AC, Kovacs CS (2013) Upregulation of calcitriol during pregnancy and skeletal recovery after lactation do not require parathyroid hormone. J Bone Miner Res 28: 1987-2000
28. Chong WH, Andreopoulou P, Chen CC, Reynolds J, Guthrie L, Kelly M, Gafni RI, Bhattacharyya N, Boyce AM, El-Maouche D, et al. (2013) Tumor localization and biochemical response to cure in tumor-induced osteomalacia. J Bone Miner Res 28: 1386-1398
29. Parekh AB (2010) Store-operated CRAC channels: function in health and disease. Nat Rev Drug Discov 9: 399-410
30. Prakriya M, Feske S, Gwack Y, Srikanth S, Rao A, Hogan PG (2006) Orai1 is an essential pore subunit of the CRAC channel. Nature 443: 230-233
31. Peinelt C, Vig M, Koomoa DL, Beck A, Nadler MJ, Koblan-Huberson M, Lis A, Fleig A, Penner R, Kinet JP (2006) Amplification of CRAC current by STIM1 and CRACM1 (Orai1). Nat Cell Biol 8: 771-773
32. Lang F, Shumilina E (2013) Regulation of ion channels by the serum- and glucocorticoid-inducible kinase SGK1. FASEB J 27: 3-12
33. Terada Y, Ueda S, Hamada K, Shimamura Y, Ogata K, Inoue K, Taniguchi Y, Kagawa T, Horino T, Takao T (2012) Aldosterone stimulates nuclear factor-kappa B activity and

transcription of intercellular adhesion molecule-1 and connective tissue growth factor in rat mesangial cells via serum- and glucocorticoid-inducible protein kinase-1. Clin Exp Nephrol 16: 81-88
34. Zhu CJ, Wang QQ, Zhou JL, Liu HZ, Hua F, Yang HZ, Hu ZW (2012) The mineralocorticoid receptor-p38MAPK-NFkappaB or ERK-Sp1 signal pathways mediate aldosterone-stimulated inflammatory and profibrotic responses in rat vascular smooth muscle cells. Acta Pharmacol Sin 33: 873-878
35. Tang WJ, Wang LF, Xu XY, Zhou Y, Jin WF, Wang HF, Gao J (2010) Autocrine/paracrine action of vitamin D on FGF23 expression in cultured rat osteoblasts. Calcif Tissue Int 86: 404-410
36. Vallon V, Wyatt AW, Klingel K, Huang DY, Hussain A, Berchtold S, Friedrich B, Grahammer F, Belaiba RS, Gorlach A, et al. (2006) SGK1-dependent cardiac CTGF formation and fibrosis following DOCA treatment. J Mol Med (Berl) 84: 396-404
37. Lang F, Eylenstein A, Shumilina E (2012) Regulation of Orai1/STIM1 by the kinases SGK1 and AMPK. Cell Calcium 52: 347-354
38. Tang C, Pathare G, Michael D, Fajol A, Eichenmuller M, Lang F (2011) Downregulation of Klotho expression by dehydration. Am J Physiol Renal Physiol 301: F745-750
39. Lang F, Ritz E, Voelkl J, Alesutan I (2013) Vascular calcification--is aldosterone a culprit? Nephrol Dial Transplant 28: 1080-1084
40. Ma TK, Szeto CC (2012) Mineralocorticoid receptor antagonist for renal protection. Ren Fail 34: 810-817
41. Ritz E, Koleganova N, Piecha G (2011) Is there an obesity-metabolic syndrome related glomerulopathy? Curr Opin Nephrol Hypertens 20: 44-49
42. Mihailidou AS (2012) Aldosterone in heart disease. Curr Hypertens Rep 14: 125-129
43. Sarraf M, Masoumi A, Schrier RW (2009) Cardiorenal syndrome in acute decompensated heart failure. Clin J Am Soc Nephrol 4: 2013-2026
44. Schrier RW (2006) Water and sodium retention in edematous disorders: role of vasopressin and aldosterone. Am J Med 119: S47-53
45. Schrier RW, Masoumi A, Elhassan E (2010) Aldosterone: role in edematous disorders, hypertension, chronic renal failure, and metabolic syndrome. Clin J Am Soc Nephrol 5: 1132-1140
46. Lang F, Bohmer C, Palmada M, Seebohm G, Strutz-Seebohm N, Vallon V (2006) (Patho)physiological significance of the serum- and glucocorticoid-inducible kinase isoforms. Physiol Rev 86: 1151-1178
47. Pathare G, Foller M, Michael D, Walker B, Hierlmeier M, Mannheim JG, Pichler BJ, Lang F (2012) Enhanced FGF23 Serum Concentrations and Phosphaturia in Gene Targeted Mice Expressing WNK-Resistant Spak. Kidney Blood Press Res 36: 355-364
48. Pathare G, Foller M, Daryadel A, Mutig K, Bogatikov E, Fajol A, Almilaji A, Michael D, Stange G, Voelkl J, et al. (2012) OSR1-Sensitive Renal Tubular Phosphate Reabsorption. Kidney Blood Press Res 36: 149-161
49. Gattineni J, Twombley K, Goetz R, Mohammadi M, Baum M (2011) Regulation of Serum 1,25(OH)2Vitamin D3 levels by Fibroblast Growth Factor 23 is Mediated by FGF Receptors 3 and 4. Am J Physiol Renal Physiol 301: F371-F377
50. Shimada T, Yamazaki Y, Takahashi M, Hasegawa H, Urakawa I, Oshima T, Ono K, Kakitani M, Tomizuka K, Fujita T, et al. (2005) Vitamin D receptor-independent FGF23 actions in regulating phosphate and vitamin D metabolism. Am J Physiol Renal Physiol 289: F1088-F1095
51. London GM, Guerin AP, Marchais SJ, Metivier F, Pannier B, Adda H (2003) Arterial media calcification in end-stage renal disease: impact on all-cause and cardiovascular mortality. Nephrol Dial Transplant 18: 1731-1740

52. Rodriguez M, Martinez-Moreno JM, Rodriguez-Ortiz ME, Munoz-Castaneda JR, Almaden Y (2011) Vitamin D and vascular calcification in chronic kidney disease. Kidney Blood Press Res 34: 261-268
53. Kuro-o M (2010) Klotho. Pflugers Arch 459: 333-343
54. Bernheim J, Benchetrit S (2011) The potential roles of FGF23 and Klotho in the prognosis of renal and cardiovascular diseases. Nephrol Dial Transplant 26: 2433-2438
55. Shalhoub V, Shatzen EM, Ward SC, Davis J, Stevens J, Bi V, Renshaw L, Hawkins N, Wang W, Chen C, et al. (2012) FGF23 neutralization improves chronic kidney disease-associated hyperparathyroidism yet increases mortality. J Clin Invest 122: 2543-2553

Figure Legends

Fig. 1. Effect of aldosterone on the FGF23 serum level

A. Arithmetic means ± SEM (n=9-11) of serum FGF23 concentrations in wild type mice sham-treated (white bar) or treated with a single DOCA injection (100 mg/kg b.w. s.c.) for 12 hrs (black bar).

B. Arithmetic means ± SEM (n=11) of serum FGF23 concentrations in wild type mice treated with normal diet (white bar) or with low salt diet for 14 days (black bar).

C. Arithmetic means ± SEM (n=4-5) of the relative Fgf23 mRNA abundance in wild type mice sham-treated (white bar) or treated with a single DOCA injection (100 mg/kg b.w. s.c.) for 12 hrs (black bar). *($p<0.05$), **($p<0.001$), ***($p<0.001$), indicate significant difference.

Fig. 2 Expression of Orai1 in bone, osteoblasts, UMR106 cells, and the effect of NFκB inhibitor wogonin

A. Original Western blots showing the protein expression of Orai1 (1st lane) and GAPDH (2nd lane), in UMR106 cells (UMR), immortalized primary periosteal cells (IPO) and bone.

B. Original 2% agarose gel showing specific amplification of Orai1 (357 bp), Orai2 (292 bp), Orai3 (328 bp), Stim1 (163 bp), Stim2 (298 bp) and Tbp (91 bp) cDNA in UMR106 cells.

C. Arithmetic means ± SEM (n=9) of Orai1 mRNA abundance (relative to Tbp mRNA) in UMR106 cells incubated without (white bar) or with (black bar) NFκB inhibitor wogonin (100 μM, 48 h). ***($p<0.001$), indicate significant difference

Fig. 3. Effect of 2-APB, YM58483, Orai1 silencing, and wogonin on SOCE in UMR106 cells

A,D,J. Representative original tracings showing intracellular Ca^{2+} concentrations ($[Ca^{2+}]_i$) in Fura-2/AM loaded UMR106 cells prior to and following removal of extracellular Ca^{2+}, addition of the sarco-endoplasmic Ca^{2+} ATPase (SERCA) inhibitor thapsigargin (1 μM) and readdition of extracellular Ca^{2+}, all in the absence (open circles) and presence (closed circles) of Orai inhibitor 2-APB (A, 50 μM), Orai inhibitor YM58483 (D, 100 nM), or NFκB inhibitor wogonin (J, 100 μM, 48 h).

B,C,E,F,H,I. Arithmetic means ± SEM of the peak (left) and slope (right) values of $[Ca^{2+}]_i$ increase following addition of thapsigargin reflecting Ca^{2+} release from intracellular stores (**B,E,K**) and of $[Ca^{2+}]_i$ increase following readdition of extracellular Ca^{2+} reflecting store operated Ca^{2+} entry (**C,F,L**) in UMR106 cells incubated without (white bars) or with (black bars) Orai

inhibitor 2-APB (**B-C**, 50 µM, n=22-60), or with the Orai inhibitor YM58483 (**E-F**, 100 nM, n=40-39) or the NFκB inhibitor wogonin (**K-L**, 100 µM, 48 h, n=12-31),

G. Representative original tracings showing intracellular Ca^{2+} concentrations ($[Ca^{2+}]_i$) in Fura-2/AM loaded UMR106 cells prior to and following removal of extracellular Ca^{2+}, addition of the sarco-endoplasmic Ca^{2+} ATPase (SERCA) inhibitor thapsigargin (1 µM) and readdition of extracellular Ca^{2+}, all in cells treated with unspecific siRNA (open circles) or with specific siRNA targeting Orai1 (closed circles).

H,I. Arithmetic means ± SEM of the peak (left) and slope (right) values of $[Ca^{2+}]_i$ increase following addition of thapsigargin reflecting Ca^{2+} release from intracellular stores (**H**) and of $[Ca^{2+}]_i$ increase following readdition of extracellular Ca^{2+} reflecting store operated Ca^{2+} entry (**I**) in UMR106 cells treated with unspecific siRNA (white bars) or with specific siRNA targeting Orai1 (black bars).**(p<0.001), ***(p<0.001), indicate significant difference.

Fig. 4. Effect of ionomyin, thapsigargin, 2-APB, YM58483, SK&F96365, and Orai1 silencing on FGF23 transcript levels in UMR106 cells

Arithmetic means ± SEM of Fgf23 mRNA abundance (relative to Tbp mRNA) in UMR106 cells incubated without (white bars) or with (black bars) ionomycin (**A**, 100 nM, 2 h, n=12), thapsigargin (**B**, 500 nM, 2 h, n=12), the Orai inhibitor 2-ABP (**C**, 50 µM, 24, n=6), the Orai inhibitor YM58483 (**D**, 100 nM, 24 h, n=15) and the Orai inhibitor SK&F96365 (**E**, 10 µM, 24 h, n=16-19).

F. Arithmetic means ± SEM (n=16) of Fgf23 mRNA abundance (relative to Tbp mRNA) in UMR106 cells treated with control siRNA (siNeg, white bar) or with specific Orai1 siRNA (siOrai1, black bar).*(p<0.05), **(p<0.001), ***(p<0.001) indicate significant difference (t-test).

Fig. 5. Effect of wogonin and withaferin A on Fgf23 transcript levels in UMR106 cells

Arithmetic means ± SEM of Fgf23 mRNA abundance (relative to Tbp mRNA) in UMR***106*** cells incubated without (white bars) or with (black bars) wogonin (**A**, 100 µM, 48 h, n=8-9) and withaferin A (**B**, 500 nM, 24 h, n=15-20).**(p<0.001), ***(p<0.001) indicate significant difference (t-test).

Fig. 6. Effect of aldosterone and spironolactone on SOCE

A,D. Representative original tracings showing intracellular Ca^{2+} concentrations ($[Ca^{2+}]_i$) in Fura-2/AM loaded UMR***106*** cells prior to and following removal of extracellular Ca^{2+}, addition of

the sarco-endoplasmic Ca^{2+} ATPase (SERCA) inhibitor thapsigargin (1 µM) and readdition of extracellular Ca^{2+}, all in the absence (open circles) and presence (closed circles) of aldosterone (**A**, 100 nM, 24 h), or spironolactone (**D**, 10 µM, 24 h).

B,C,E,F. Arithmetic means ± SEM of the peak (left) and slope (right) values of $[Ca^{2+}]_i$ increase following addition of thapsigargin reflecting Ca^{2+} release from intracellular stores (**B,E**) and of $[Ca^{2+}]_i$ increase following readdition of extracellular Ca^{2+} reflecting store operated Ca^{2+} entry (**C,F**) in UMR106 cells incubated without (white bars) or with (black bars) aldosterone (**B-C**, 100 nM, 24 h, n=72-80), or spironolactone (**E-F**, 10 µM, 24 h, n=121-133）. *(p<0.05), ***(p<0.001) indicate significant difference (t-test).

Fig.7. Effect of aldosterone on FGF23 transcript levels in UMR106 cells with or without presence of spironolactone, eplerenone, YM58483 and withaferin A

A. Arithmetic means ± SEM (n=18) of Orai1 mRNA abundance (relative to Tbp mRNA) in UMR***106*** cells incubated without (white bar) or with (black bar) aldosterone (100 nM, 24 h).

B. Arithmetic means ± SEM (n=7) of FGF23 mRNA abundance (relative to Tbp mRNA) in UMR***106*** cells incubated without (white bars) or with (black bars) aldosterone (100 nM, 6 h) in the absence (left bars) or presence (right bars) of spironolactone (10 µM) of Orai inhibitor YM58483 (100 nM) or of NFκB inhibitor withaferin A (500 nM).

C. Arithmetic means ± SEM (n=36-37) of FGF23 mRNA abundance (relative to Tbp mRNA) in UMR***106*** cells incubated without (white bars) or with (black bars) aldosterone (6 h) at the indicated concentration.

D. Arithmetic means ± SEM (n=11) of FGF23 mRNA abundance (relative to Tbp mRNA) in UMR***106*** cells incubated without (white bars) or with (black bars) aldosterone (100 nM, 6 h) in the absence (left bars) or presence (right bars) of eplerenone (10 µM).

E. Original immunofluorescence images demonstrating nuclear staining (Draq5; Red; left images), p65-specific staining (NFκB; Green middle images), and an overlay of both, nuclear and p65-specific staining (right images) in UMR106 cells incubated without (upper images) or with (lower images) aldosterone (100 nM, 24 h) Scale bar: 20 µm.

F. Arithmetic means ± SEM (n=12) of FGF23 mRNA abundance (relative to Tbp mRNA) in UMR106 cells incubated without (white bars) or with (black bars) aldosterone (100 nM, 6 h) in the absence (left bars) or presence (right bars) of SGK1 inhibitor EMD638683 (50 µM).

*, **, *** (p<0.05, p<0.01, p<0.001) indicate difference from control. ### (p<0.001) indicates difference from aldosterone alone.

Fig.8. Dose response relationship of mineralocorticoid and glucocorticoid antagonism with the aldosterone effect on FGF23 transcription

Arithmetic means ± SEM of FGF23 mRNA abundance (relative to Tbp mRNA) in UMR106 cells incubated with spironolactone (**A**; n=15), eplerenone (**B**; n=9-11), or mifepristone (**C**; n= 4-6) at the indicated concentration without (white bars) or with (black bars) 100 nM aldosterone (6 h).

*, ** ($p<0.05$, $p<0.01$) indicate difference from control. #, ### ($p<0.05$, $p<0.001$) indicate difference from aldosterone alone.

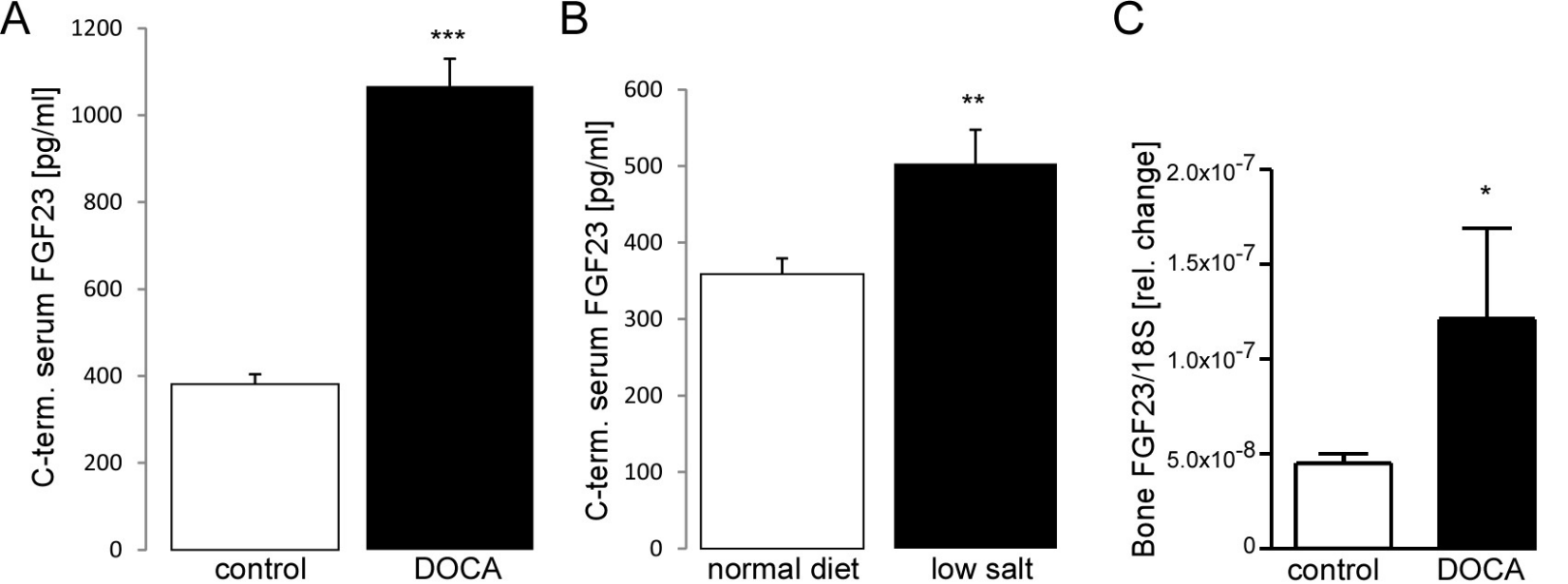
A
C-term. serum FGF23 [pg/ml]
1200
1000
800
600
400
200
0
***
control
DOCA
B
C-term. serum FGF23 [pg/ml]
600
500
400
300
200
100
0
**
normal diet
low salt
C
Bone FGF23/18S [rel. change]
2.0x10-7
1.5x10-7
1.0x10-7
5.0x10-8
0
*
control
DOCA

Figure 1

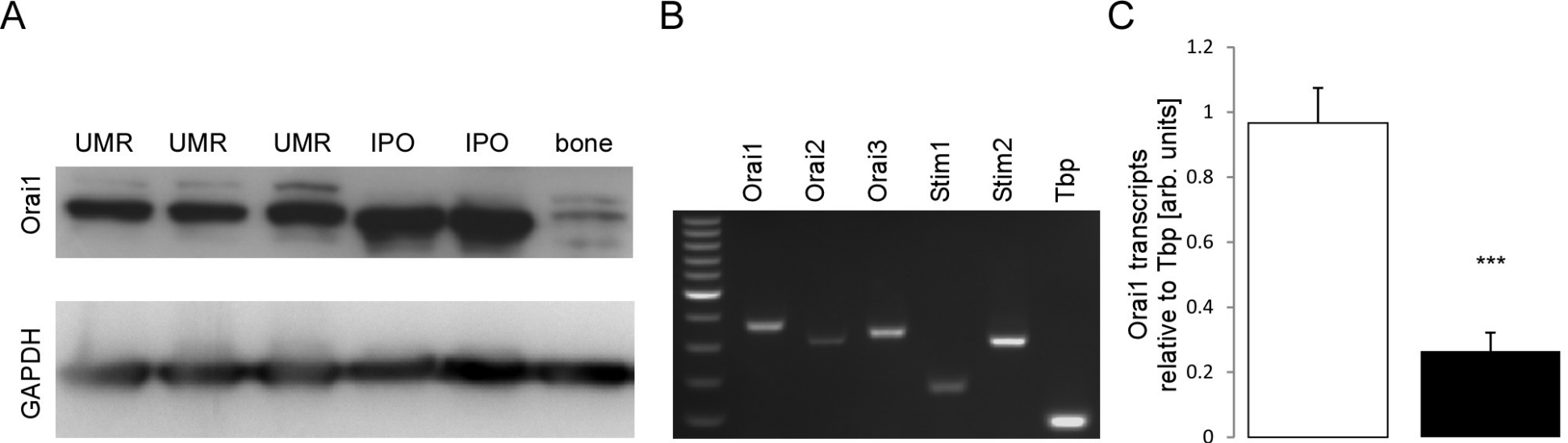
A
UMR
UMR
UMR
IPO
IPO
bone
Orai1
GAPDH
B
Orai1
Orai2
Orai3
Stim1
Stim2
Tbp
C
Orai1 transcripts relative to Tbp [arb. units]
1.2
1
0.8
0.6
0.4
0.2
0
***
control
wogonin

Figure 2

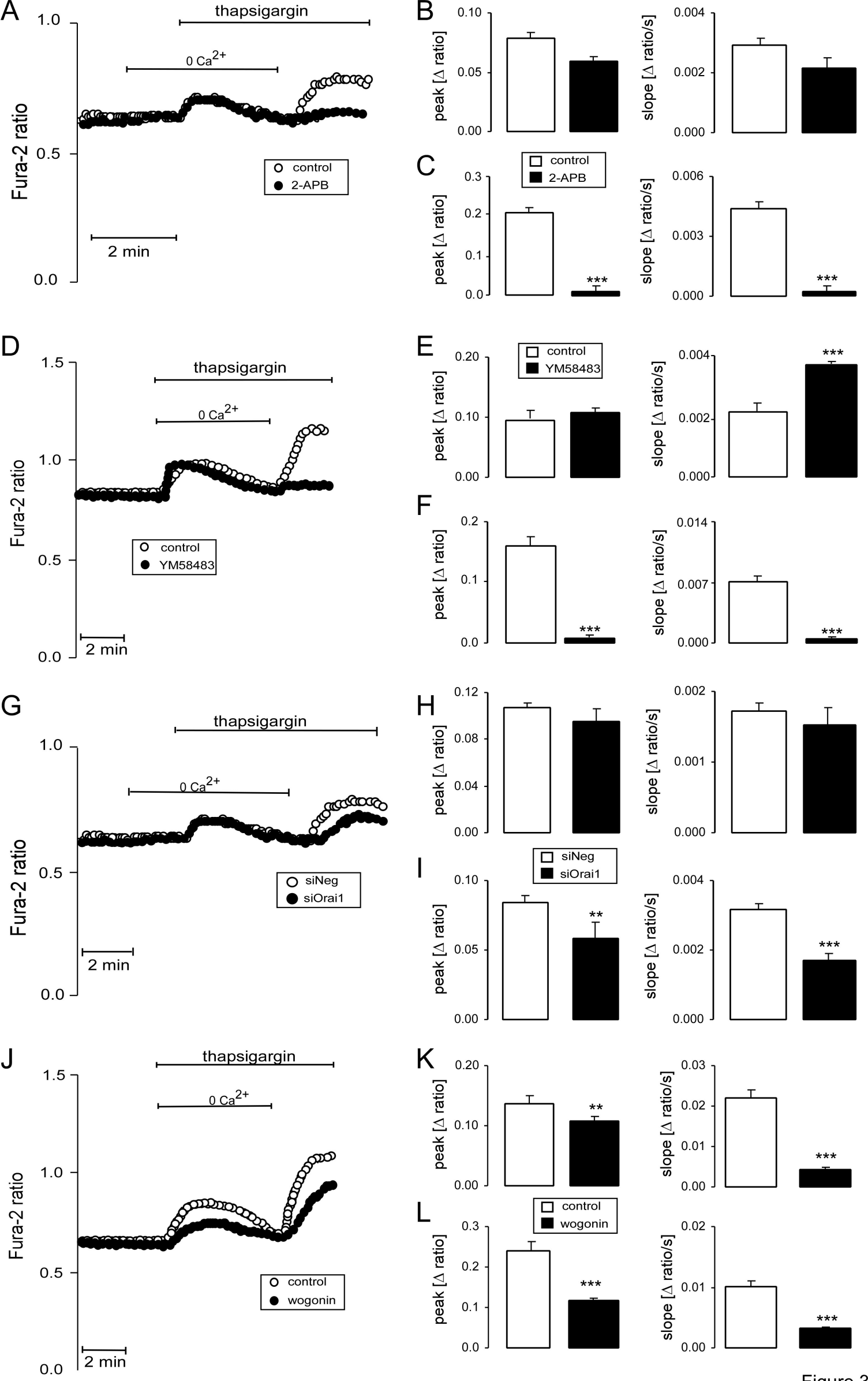
A
thapsigargin
0 Ca2+
Fura-2 ratio
control
2-APB
2 min
B
peak [Δ ratio]
slope [Δ ratio/s]
C
control
2-APB
***
D
thapsigargin
0 Ca2+
Fura-2 ratio
control
YM58483
2 min
E
control
YM58483
***
F
***
G
thapsigargin
0 Ca2+
Fura-2 ratio
siNeg
siOrai1
2 min
H
I
siNeg
siOrai1
**
***
J
thapsigargin
0 Ca2+
Fura-2 ratio
control
wogonin
2 min
K
**
***
L
control
wogonin
***

Figure 3

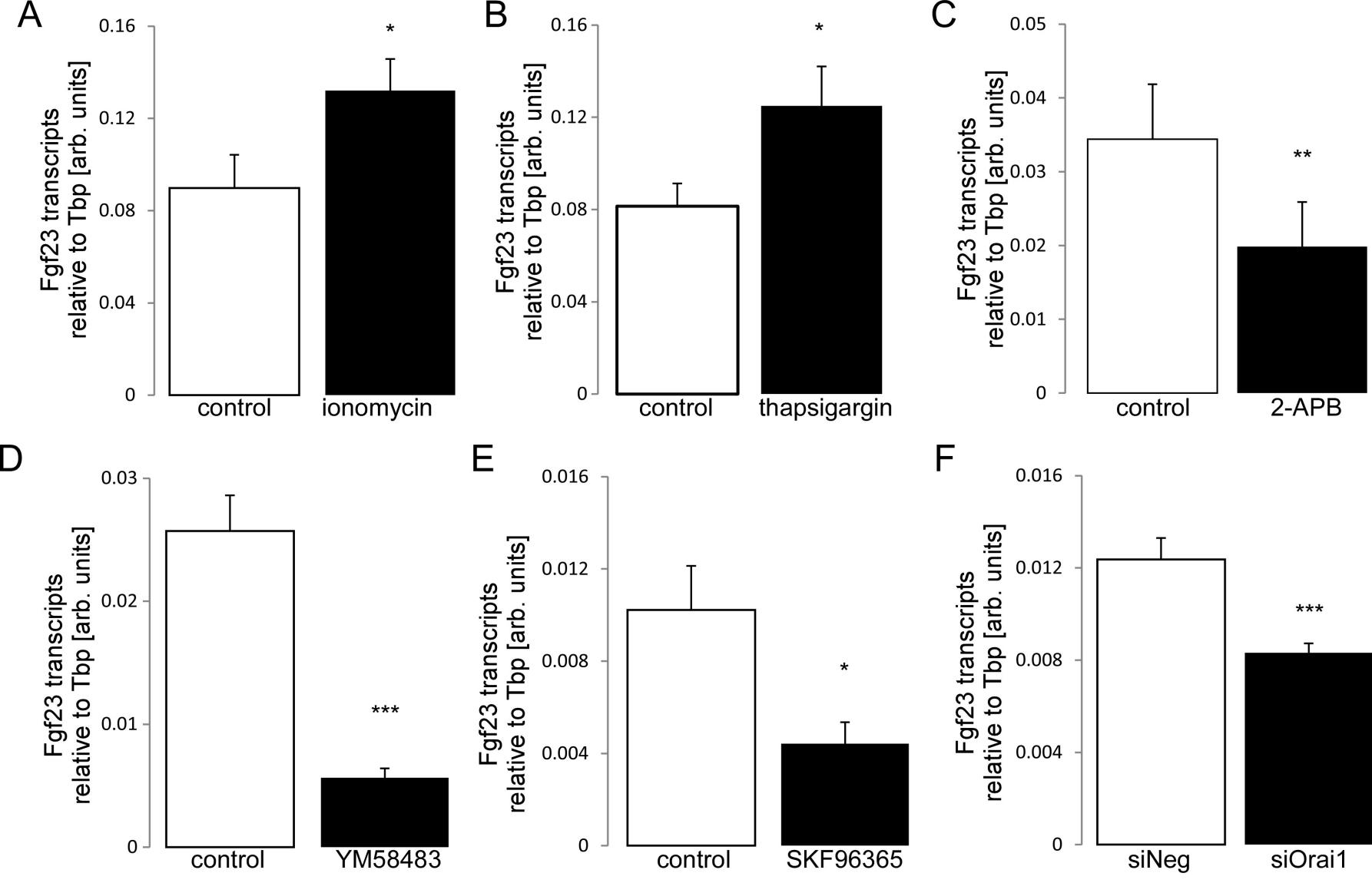
A
Fgf23 transcripts relative to Tbp [arb. units]
0.16
0.12
0.08
0.04
0
*
control
ionomycin
B
Fgf23 transcripts relative to Tbp [arb. units]
0.16
0.12
0.08
0.04
0
*
control
thapsigargin
C
Fgf23 transcripts relative to Tbp [arb. units]
0.05
0.04
0.03
0.02
0.01
0
**
control
2-APB
D
Fgf23 transcripts relative to Tbp [arb. units]
0.03
0.02
0.01
0
***
control
YM58483
E
Fgf23 transcripts relative to Tbp [arb. units]
0.016
0.012
0.008
0.004
0
*
control
SKF96365
F
Fgf23 transcripts relative to Tbp [arb. units]
0.016
0.012
0.008
0.004
0
***
siNeg
siOrai1

Figure 4

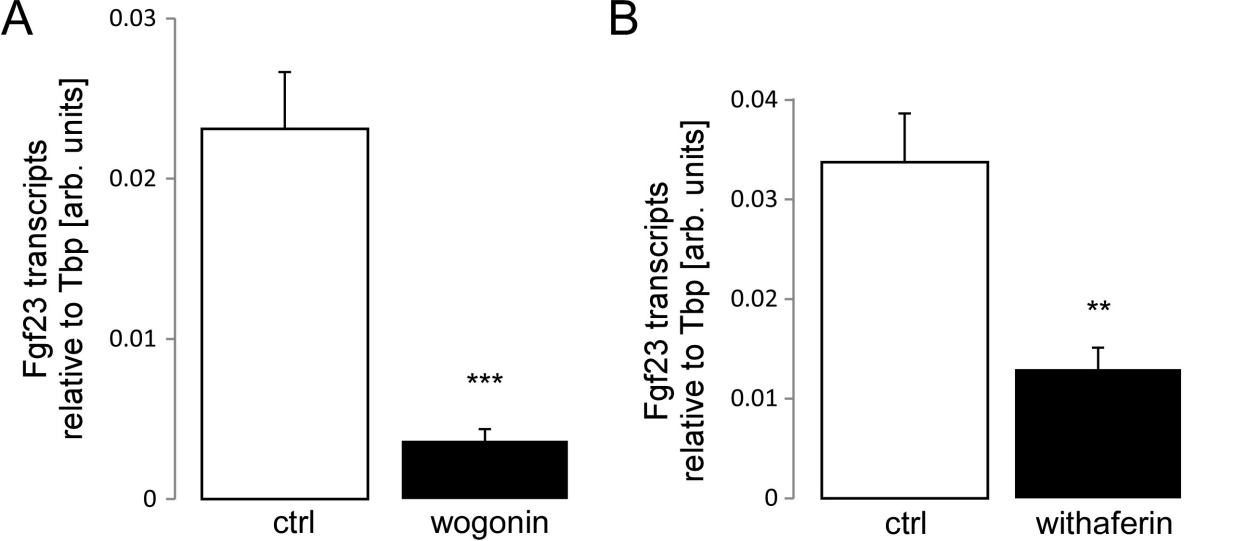
A
0.03
0.02
0.01
0
Fgf23 transcripts
relative to Tbp [arb. units]
***
ctrl
wogonin
B
0.04
0.03
0.02
0.01
0
Fgf23 transcripts
relative to Tbp [arb. units]
**
ctrl
withaferin

Figure 5

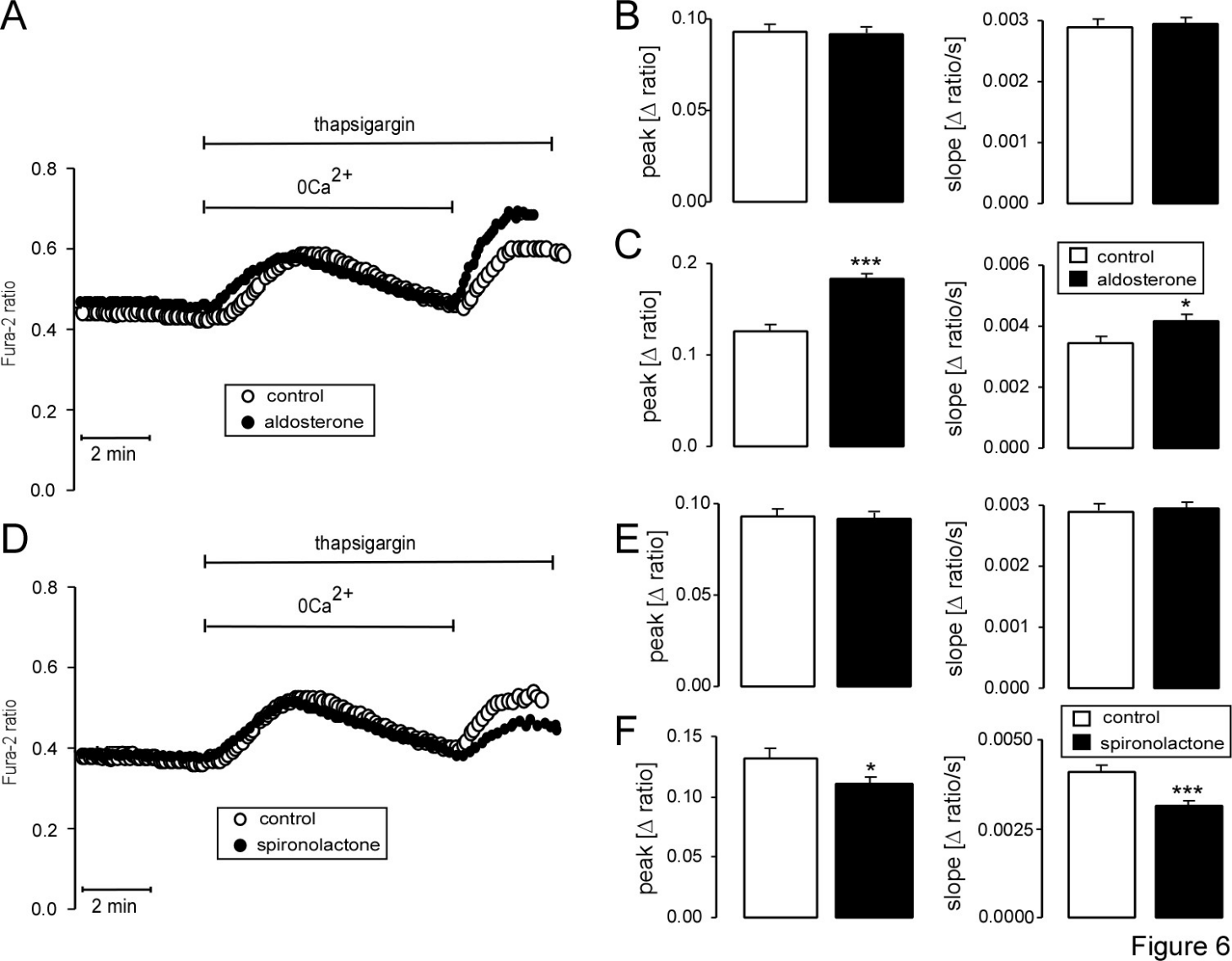
A
thapsigargin
0Ca2+
Fura-2 ratio
0.8
0.6
0.4
0.2
0.0
control
aldosterone
2 min
B
peak [Δ ratio]
0.10
0.05
0.00
slope [Δ ratio/s]
0.003
0.002
0.001
0.000
C
***
control
aldosterone
*
0.2
0.1
0.0
0.006
0.004
0.002
0.000
D
thapsigargin
0Ca2+
Fura-2 ratio
control
spironolactone
2 min
E
F
*
***
control
spironolactone
0.15
0.10
0.05
0.00
0.0050
0.0025
0.0000

Figure 6

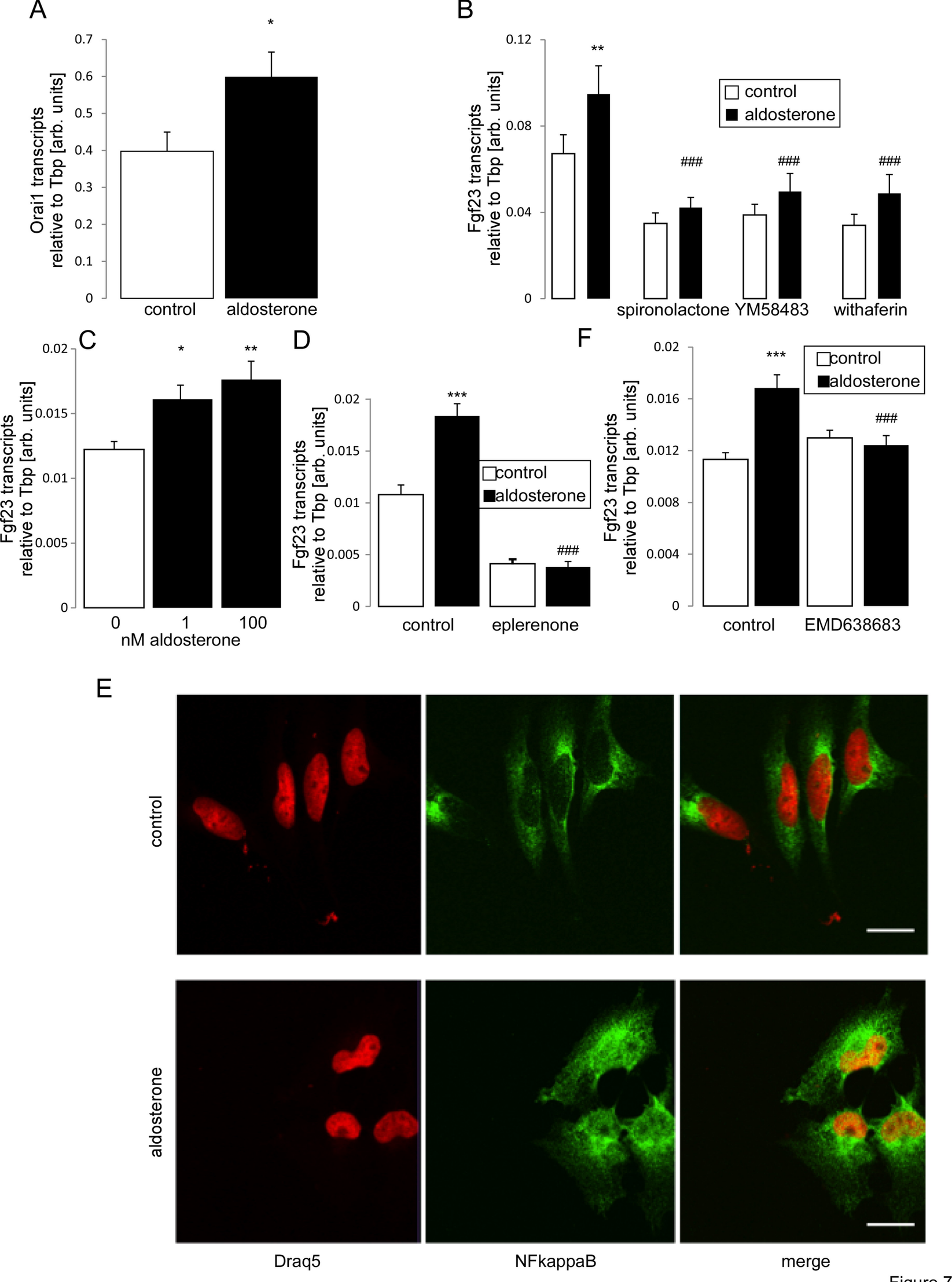
A
Orai1 transcripts relative to Tbp [arb. units]
0.7
0.6
0.5
0.4
0.3
0.2
0.1
0
*
control
aldosterone
B
Fgf23 transcripts relative to Tbp [arb. units]
0.12
0.08
0.04
0
**
control
aldosterone
###
###
###
spironolactone
YM58483
withaferin
C
Fgf23 transcripts relative to Tbp [arb. units]
0.02
0.015
0.01
0.005
0
*
**
0
1
100
nM aldosterone
D
Fgf23 transcripts relative to Tbp [arb. units]
0.02
0.015
0.01
0.005
0
***
control
aldosterone
###
control
eplerenone
F
Fgf23 transcripts relative to Tbp [arb. units]
0.02
0.016
0.012
0.008
0.004
0
***
control
aldosterone
###
control
EMD638683
E
control
aldosterone
Draq5
NFkappaB
merge

Figure 7

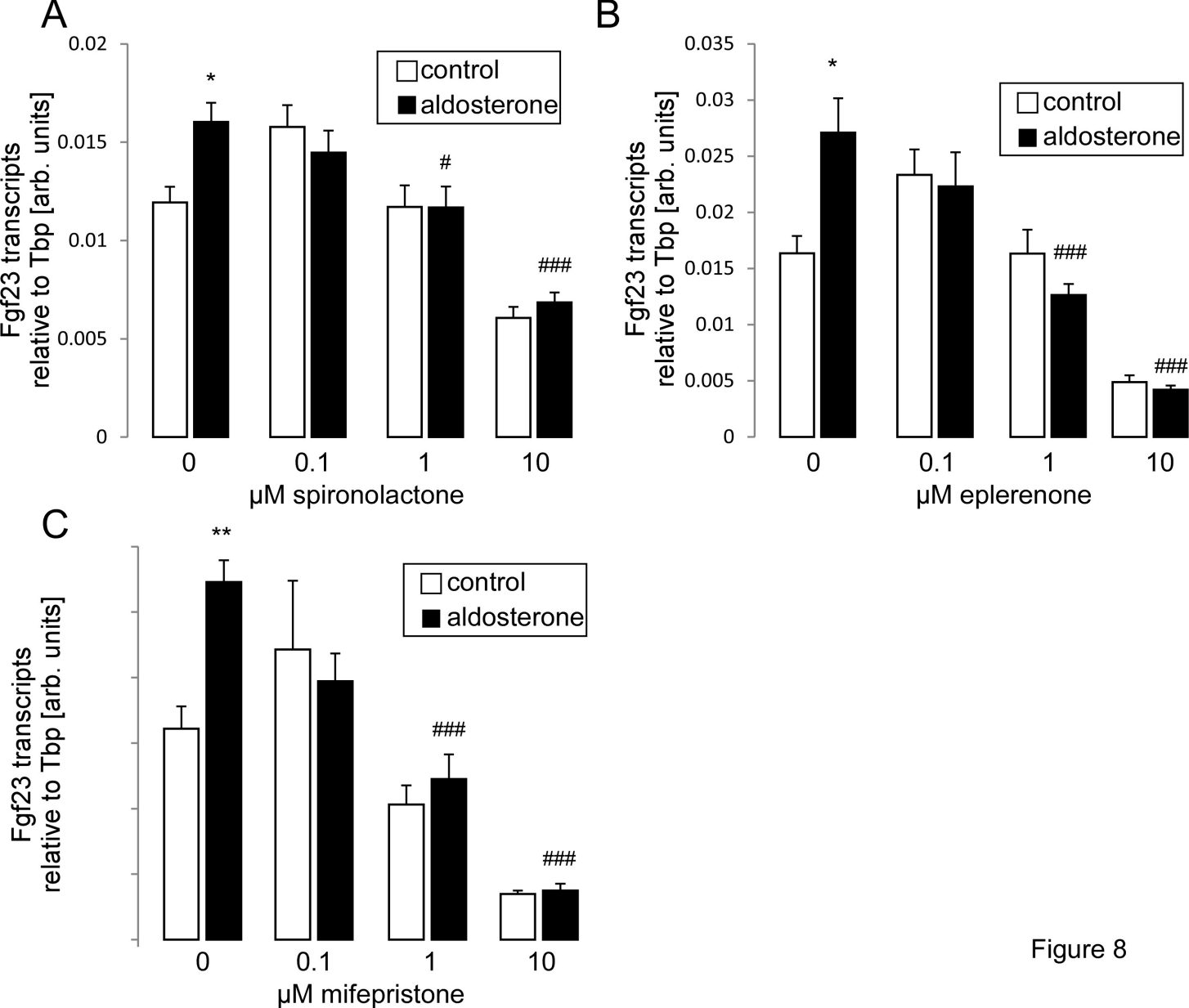
A
0.02
0.015
0.01
0.005
0
Fgf23 transcripts relative to Tbp [arb. units]
control
aldosterone
*
#
###
0
0.1
1
10
µM spironolactone
B
0.035
0.03
0.025
0.02
0.015
0.01
0.005
0
Fgf23 transcripts relative to Tbp [arb. units]
control
aldosterone
*
###
###
0
0.1
1
10
µM eplerenone
C
Fgf23 transcripts relative to Tbp [arb. units]
control
aldosterone
**
###
###
0
0.1
1
10
µM mifepristone

Figure 8

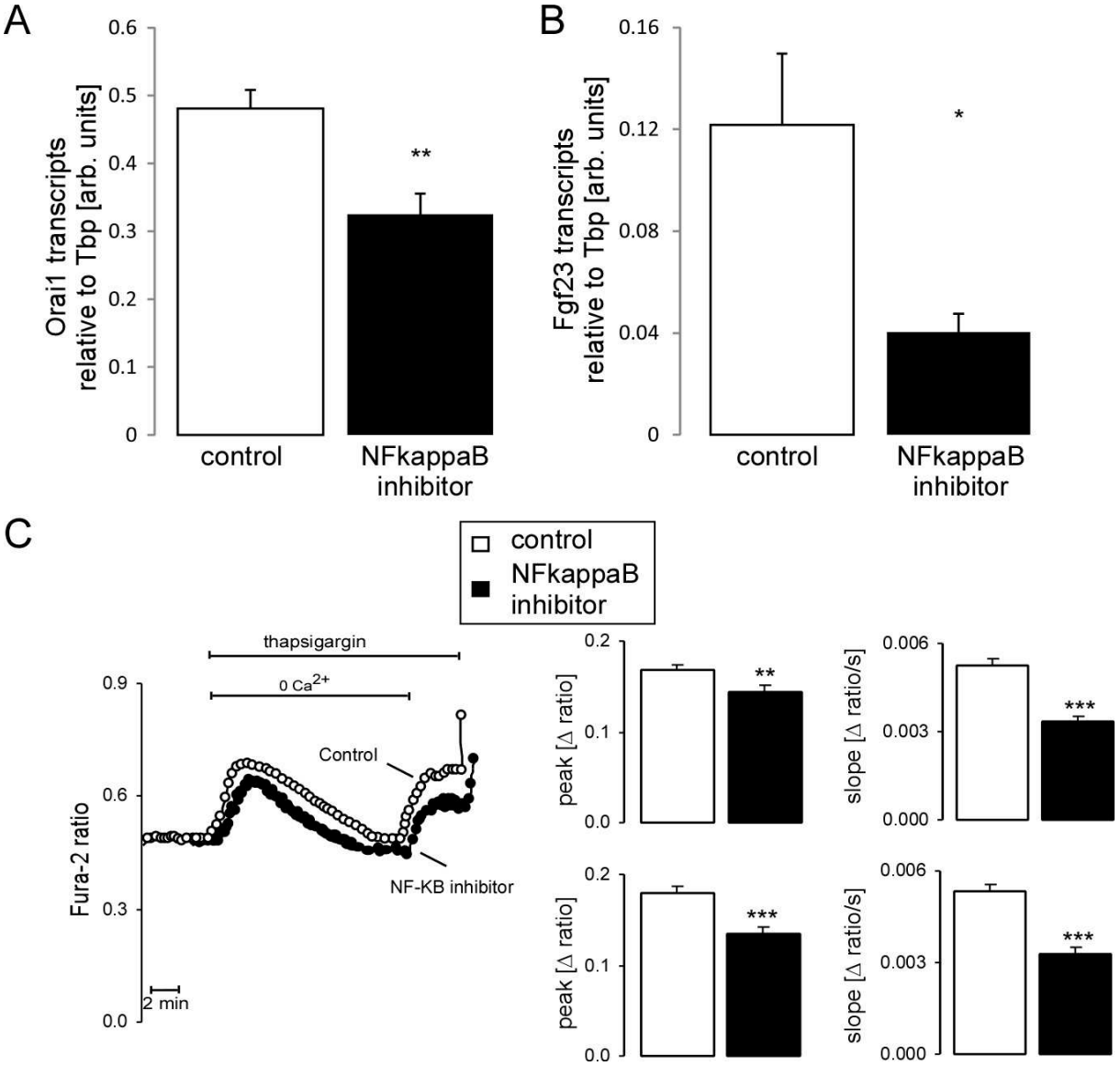

Suppl. Fig 1. **NFκB inhibitor** ***CAS 545380-34-5 lowers Orai1 and FGF23 transcript levels as well as SOCE in UMR106 cells***

A. Arithmetic means ± SEM (n=6) of Orai1 mRNA abundance (relative to Tbp mRNA) in UMR106 cells incubated without or with NFκB inhibitor CAS 545380-34-5 (100 nM, 24 h).

B. Arithmetic means ± SEM (n=6) of FGF23 mRNA abundance (relative to Tbp mRNA) in UMR cells incubated without or with NFκB inhibitor CAS 545380-34-5 (100 nM, 24 h).

C. Representative original tracings (left panel) showing intracellular Ca^{2+} concentrations ($[Ca^{2+}]_i$) in Fura-2/AM loaded UMR106 cells prior to and following removal of extracellular Ca^{2+}, addition of the sarco-endoplasmic Ca^{2+} ATPase (SERCA) inhibitor thapsigargin (1 µM) and readdition of extracellular Ca^{2+} in the absence (open circles) and presence (closed circles) of the NFκB inhibitor CAS 545380-34-5 (100 nM, 24 h). The upper right panel depicts the arithmetic means ± SEM (n=45-72) of the peak (left) and slope (right) values of $[Ca^{2+}]_i$ increase following addition of thapsigargin reflecting Ca^{2+} release from intracellular stores and the lower right shows the arithmetic means ± SEM (n=45-72) of the peak (left) and slope (right) values of $[Ca^{2+}]_i$ increase following readdition of extracellular Ca^{2+} reflecting store operated Ca^{2+} entry in UMR106 cells incubated without (white bars) or with (black bars) NFκB inhibitor CAS 545380-34-5 (100 nM, 24 h).

(p<0.01), *(p<0.001) indicate significant difference (t-test).